PRE-PRINT ARTICLE

COPYRIGHT BY COMPOSITES THEORY AND PRACTICE JOURNAL

ISSN: 2299-128X

Alternative holder design for thick specimens intended for compressive strength testing of UD composites

Piotr Czarnocki
Warsaw University of Technology,
Institute of Aeronautics and Applied Mechanics,
Nowowiejska 24, Warsaw, Poland
piotr.czarnocki@pw.edu.pl
[0000-0002-0620-6654]

https://doi.org/10.62753/ctp.2026.01.1.1

Index of non-standard abbreviations

ESC - end stress concentration
ESCF - end stress concentration factor
HDN - holder design number
IHD - intermediate holder design
ISRI - inverse strength ratio index
MPSC - meniscus plane stress concentration
MPSCF - meniscus plane stress concentration factor
SCF - stress concentration factor

Abstract

The standard specimens used to determine the compressive strength of unidirectional (UD) composites are of a relatively small cross-section. The compressive strength of such materials depends on the volume of the tested material and decreases with its increase. Therefore, the results of tests carried out using such specimens may have limited applicability to the design of actual structures, and larger ones should replace standard-sized specimens.

The performance of a hybrid holder designed for non-standard specimens of relatively large cross-sections, intended to determine the compressive strength of UD composites, was investigated numerically. Selected numerical results were compared against preexisting experimental data.

The holder consisted of a metal cup filled with resin surrounding a specimen. The results showed that (i) concentrations of longitudinal stress occurred in two locations: at the tip of the specimen touching the bottom of the cup and in the resin meniscus plane, (ii) the proportion between them could be controlled by (a) the presence or absence of adhesion between the resin and specimen, and the resin and cup wall, (b) by friction at the mentioned interfaces, and (c) by the specimen immersion depth. Eliminating adhesion and friction at the specimen/resin/cup interfaces reduced the differences in the values of the stress concentration factor present at the end of the specimen and in the meniscus plane, indicating the possibility of optimizing the holder design.

Keywords: composites, strength, tests

1. Introduction

It has been experimentally proven that the compressive strength of polymeric composites depends on the volume of the tested material [1-5], as shown in Table 1. Because the standard specimens [6-10] used to determine this property are of a relatively small cross-section, the results of tests carried out using such specimens may have limited applicability to the design of actual structures. This limitation can be particularly crucial if a structure contains large and thick cross-section elements. Figure 1 presents

PRE-PRINT ARTICLE
COPYRIGHT BY COMPOSITES THEORY AND PRACTICE JOURNAL
ISSN: 2299-128X

the cross-section corresponding to an ASTM specimen (shown in white) against the cross-section of a light aircraft's actual (crashed) spar flange.

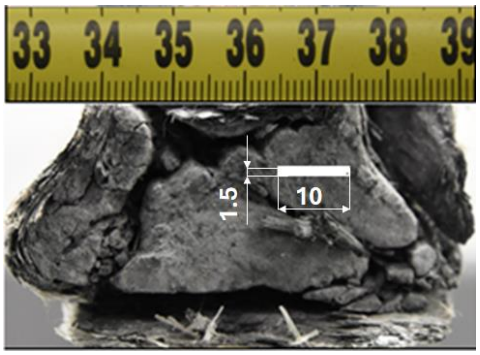

Fig. 1. ASTM D 3410 standard specimen cross-section shown to scale (in white) against flange cross-section. Ruler shown at top is metric.

The average compressive strength determined using specimens of almost the same cross-section was about 900 N/mm^2, while the spar flange failed at about 540 N/mm^2. It was important that no particular manufacturing flaws were found during the post-failure inspection that could weaken the flange.

Table 1. Effect of specimen volume or cross-section area on apparent strength

Reference	Parameter		Strength [N/mm^2]	Notice
[1]	Vol_{max} [mm^3]	41097	967	In all cases, non-standard specimens were used
	Vol_{min} [mm^3]	5129	1275	
[2]	Vol_{max} [mm^3]	183	1593	
	Vol_{min} [mm^3]	165	1684	
[3]	Vol_{max} [mm^3]	1000	500	
	Vol_{min} [mm^3]	100	1600	
[4]	Vol_{max} [mm^3]	20516	853	
	Vol_{min} [mm^3]	5169	1160	
[5]	Vol_{max} [mm^3]	12800	869	
	Vol_{min} [mm^3]	200	1570	
Author's research results	S_{max} [mm^2]	1540	540	
	S_{min} [mm^2]	16	900	

It could indicate that the results of the tests conducted using small specimens were not indicative. In such circumstances, experimental setups utilizing specimens of larger cross-sections can be more suitable [11-14]. They require holders of designs differing from those applied for standard-sized specimens. Due to the large cross-section, buckling is usually not a threat, and specimens do not require side support, making it possible to load them at the ends [6,11,12]; however, it can result in premature failure as a consequence of insufficient bearing strength. To avoid it, side tabs [13] or metal collar

PRE-PRINT ARTICLE
COPYRIGHT BY COMPOSITES THEORY AND PRACTICE JOURNAL
ISSN: 2299-128X

holders of a particular design [14] are suggested. In both standard-size and large cross-section specimens, there is a common problem of stress concentration; moreover, their values near the ends of the tabs grow with the increase in specimen cross-sections [12,15]. Yet, another specimen holder suitable for testing specimens of relatively large cross-sections could be considered, Fig. 2.

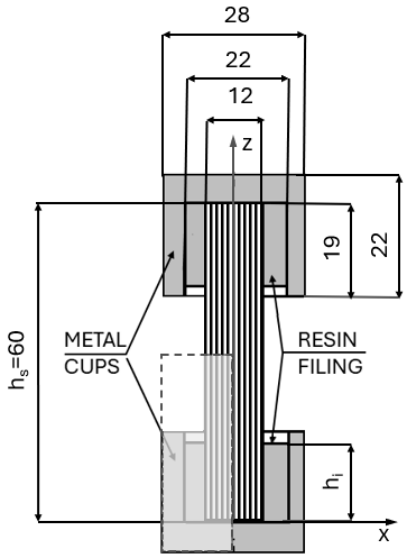

Fig. 2. Experimental setup with alternative holder. Modeled part is shaded.

It consists of metal cups filled with resin and a test piece with its ends immersed in the resin. The idea is known [16], nevertheless, to the best of the author's knowledge, it has never been investigated in detail to reveal its potential in controlling stress concentrations in compression-loaded specimens. The essentials of specimen loading are the same as those in the tests mentioned above. The specimen is loaded due to the pressure at the specimen ends and the shear at the side walls. The author believes this means of loading has two advantages over the previously mentioned one. Firstly, it is suitable for testing specimens of much larger cross-sections than those of standard ones. Secondly, an important attribute of this design is that the constraints imposed by the surrounding resin on the specimens to load them could be adjusted, affecting stress concentrations, which is very difficult to achieve using holders of standard or similar designs. In the case of the alternative holder, it can be achieved by varying the immersion depth and the adherence of the cup, resin, and specimen interfaces. The latter can be obtained by the selective application of a release agent. Further investigation showed that the amount of release agent could affect the geometry of the formed resin meniscus. It was found that a thick layer of release agent could produce a convex meniscus, Fig. 3. Surprisingly, a thin layer of the agent, still assuring a lack of adhesion at the interfaces, resulted in a concave meniscus. Its geometry was close to that of the meniscus formed when the specimen sides were clean. The friction occurring at the contacting surfaces was difficult to determine, hence limited sensitivity analyses were performed assuming friction

PRE-PRINT ARTICLE
COPYRIGHT BY COMPOSITES THEORY AND PRACTICE JOURNAL
ISSN: 2299-128X

coefficients μ=0 and μ=0.5. The assumption concerning the latter value was made based on literature data [17-20], which were in the range of 0.3-0.8.

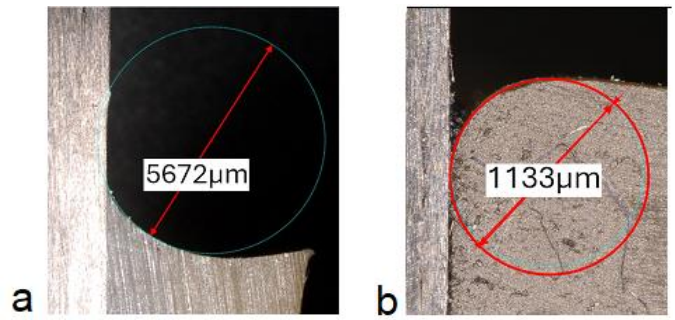

Fig. 3. Profiles of resin menisci surrounding immersed samples: (a) concave, (b) convex.

Although knowing the exact stress concentration factor (SCF) value is essential, its determination only makes sense for specific material tests where the elastic constants of the resin and the material being tested are known. Such consideration was out of the scope of the presented analysis. The investigations aimed to obtain qualitative results that gave insight into the relationships between the parameters listed below as well as stress concentrations in critical regions of the sample and the determination of these regions. The effects of the presence or lack of adhesion at the cup, resin, and specimen interfaces, different values of μ, the immersion depth, and the meniscus geometry were analyzed.

2. Methods

The analysis was carried out by means of FEM. Selected numerical results were compared against preexisting experimental data.

It was assumed that all the materials were elastic and linear. Inspection of the setup to be modeled indicated that the specimen part in the vicinities of the concave meniscus end, and the end of the specimen immersed in the resin would be challenging to model because of the expected numerical singularities around the junctions of different materials forming corners [21-23]. In such regions, increasing the mesh density does not result in reaching a constant stress but produces a rise in its value with a gradient depending on the singularity order; however, the application of FEM for such problems is acceptable [24,25]. Since the investigation aimed to obtain qualitative results serving comparison purposes, it was sufficient to maintain the same mesh geometry in the critical regions of expected high stress concentrations for all the considered cases. In addition, the existing results of previously completed compressive tests allowed limited verification of the numerical analysis results.

PRE-PRINT ARTICLE
COPYRIGHT BY COMPOSITES THEORY AND PRACTICE JOURNAL
ISSN: 2299-128X

2.1. Scope of analysis

Table 2 presents the scope of the FE analysis.

Table 2. Scope of analysis

Holder design number (HDN)	Design features
1	Lack of resin; at cup/specimen-end interface μ=0
2	Lack of resin; at cup/specimen-end interface μ =0.5
3	Lack of resin; adhesion at cup/specimen-end interface
4	Resin filling; lack of adhesion at all interfaces, and contact with μ =0, concave meniscus, h_i = 20 mm
5	Resin filling; lack of adhesion at all interfaces, and contact with μ =0.5; convex meniscus, h_i = 20 mm
6	Resin filling; lack of adhesion at all interfaces; contact with μ =0.5; concave meniscus, h_i = 20 mm
7	Resin filling; adhesion at all interfaces; concave meniscus
8	Resin filling; lack of adhesion at all interfaces; contact at cup/specimen-end interface with μ =0; at remaining ones with μ =0.5; concave meniscus, h_i = 20 mm
9	Resin filling; lack of adhesion at all interfaces; contact at cup/ specimen-end interface with μ =0; at remaining ones with μ =0.5; convex meniscus, h_i = 20 mm
10	Resin filling; adhesion at specimen/resin interface; contact at remaining interfaces with μ =0; concave meniscus, h_i = 20 mm
11	Resin filling; adhesion at specimen/resin interface; contact at remaining interfaces with μ =0; concave meniscus, h_i= 5 mm
12	Resin filling; adhesion at specimen/resin interface; contact at remaining interfaces with μ =0.5; concave meniscus, h_i= 5 mm

It should be mentioned that obtaining such smooth walls of the specimen and cup that the friction between them would be zero is very unlikely. Therefore, from a practical point of view, HDN 1 is artificial and only determines the limit for numerical investigations of the friction effects.

2.2. Modelling

The analysis was carried out by utilizing ANSYS software [26]. Owing to the symmetry of the considered setup concerning the x-y, x-z, and x-y planes, only the shaded (Fig. 2) part of the setup was modeled. The assumed mechanical properties of the specimen, resin, and cup materials are given in Table 3.

PRE-PRINT ARTICLE
COPYRIGHT BY COMPOSITES THEORY AND PRACTICE JOURNAL
ISSN: 2299-128X

Table 3. Mechanical properties of materials

UD C/Epoxy composite specimen									resin		steel	
E_x	E_y	E_z	G_{xy}	G_{xz}	G_{yz}	ν_{xy}	ν_{xy}	ν_{xy}	E	ν	E	ν
11000	11000	138000	4000	6000	6000	0.3	0.1	0.1	3600	0.35	210000	0.3
X_t	X_c	Y_t	Y_c	Z_t	Z_c	S_{12}	S_{23}	S_{31}				
30	-200	30	-200	1500	-900	80	80	80				

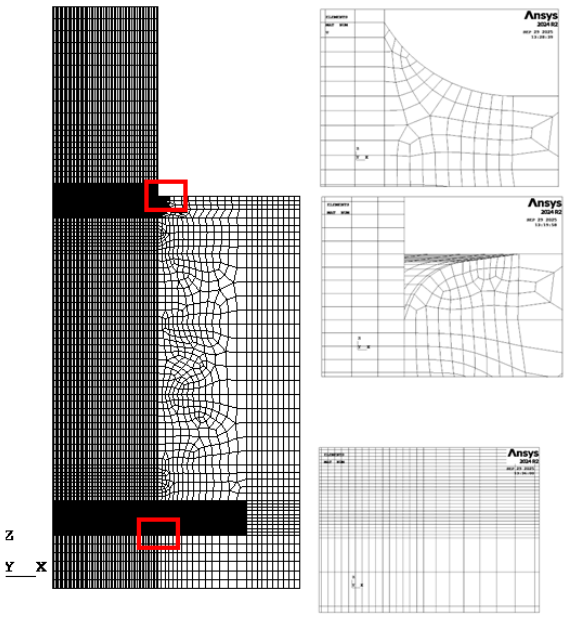

Fig. 4. FE model of setup. Pictures on right present enlargements of mesh in regions marked with red rectangle. Note that upper red rectangle indicates location of convex or concave meniscus, with its enlarged geometry shown on right.

Figure 4 shows the FE representation of the considered experimental set. The cup, resin filling, and specimen were modeled with Solid185 elements (according to the ANSYS nomenclature), for which both isotropic and orthotropic material properties could be defined. To model the contacts at the specimen-resin and resin-cup interfaces, Conta174 and Targe170 elements were employed to create surface-to-surface contact pairs. Since the exact coefficient of friction values μ for the materials covered with the release agent were unknown, the calculations were performed for μ=0 and repeated for μ=0.5. Symmetry boundary conditions were imposed on symmetry planes xz and yz, and at the xy plane for $z=h_s/2$. The specimen was loaded under displacement-controlled conditions, forcing cup bottom displacement z, which was adjusted for each considered case to produce approximately the same average stress σ_z for $z=h_s/2$.

PRE-PRINT ARTICLE
COPYRIGHT BY COMPOSITES THEORY AND PRACTICE JOURNAL
ISSN: 2299-128X

2.3. Experimental procedure

The experimental data resulted from two tests in which the specimens were loaded as shown in Fig. 5 In Setup A, the lower cup was filled with resin, and no release agent was used, enabling adhesion at all the interfaces, corresponding to HDN 7. The upper cup was empty. The clean specimen end surface was covered with a thin layer of resin to facilitate adjustment of this surface to the bottom of the cup and eliminate possible misfitting after pressing the specimen and cup against each other. A release agent was previously applied to the bottom of the cup to prevent adhesion. A tube guide was used to avoid cup misalignment. Since the coefficient of friction was unknown, it was believed that the specimen loading conditions created in this way would be intermediate regarding those offered by HDN 1 and 2, as was discussed in section 2.1. Further in the text, when analyzing the experimental results, these conditions will be referred to as intermediate, and the corresponding holder design will be referred to as IHD. In Setup B, both specimen ends were immersed in resin, filling the cups. No release agent was applied; thus, adhesion existed between all the interfaces as in the case of HDN 7. Three specimens were tested at RT using each setup.

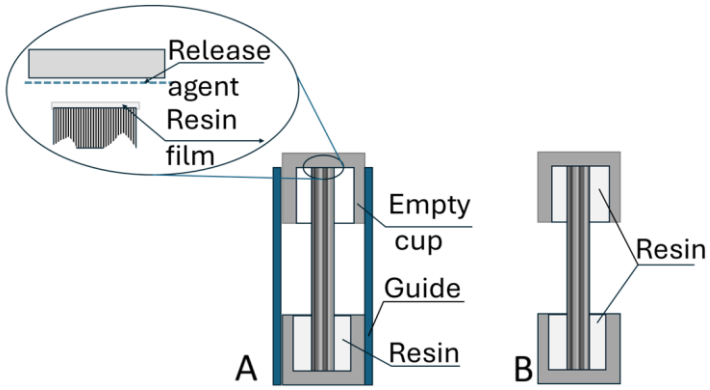

Fig. 5. Experimental setup for direct comparison of holder suitability for applying compressive load to specimen.

3. Results and discussion

3.1. Results of numerical analysis

The aggregated results of the analysis are presented in Table 4 and Figs. 6, 7 and 9. The results regarding the stress concentrations are presented in Figs. 6 and 7. They present the variation in stressing the considered specimen caused by varying the extent of adhesion at the specimen/resin/cup interfaces, resulting from the selective application of a release agent and the immersion depth of the specimen in the resin filling the cup.

PRE-PRINT ARTICLE
COPYRIGHT BY COMPOSITES THEORY AND PRACTICE JOURNAL
ISSN: 2299-128X

The SCFs were calculated based on the values of σ_z varying along the paths overlapping the specimen cylinder generator, as shown in Fig. 6. Two regions of stress concentration were detected: at the vicinity of the specimen end and the vicinity of the resin meniscus plane, Fig. 6. Hereinafter, the stress concentrations corresponding to those locations are called end stress concentration (ESC) and meniscus plane stress concentration (MPSC), respectively, and for the corresponding stress concentration factors, the short forms ESCF and MPSCF are used. The numbers assigned to each curve in Fig. 6 correspond to the HDNs defined in Table 2.

Table 4. Aggregate results of numerical analysis

HDN	σ_{zend} [N/mm^2]	σ_{zm} [N/mm^2]	ESCF	MPSCF	ISRI
1	352.38	262.17	1.34	1.00	0.40
2	605.95	246.23	2.39	1.00	0.98
3	821.89	260.20	3.16	1.00	1.11
4	352.38	279.17	1.36	1.07	0.32
5	456.37	379.45	1.75	1.43	0.60
6	405.82	342.37	1.56	1.31	0.57
7	348.39	413.47	1.34	1.59	0.58
8	253.53	340.95	0.98	1.32	0.35
9	277.03	415.42	1.06	1.59	0.46
10	336.97	382.43	1.29	1.47	0.40
11	357.92	370.64	1.37	1.42	0.37
12	499.00	507.33	1.89	1.92	0.72

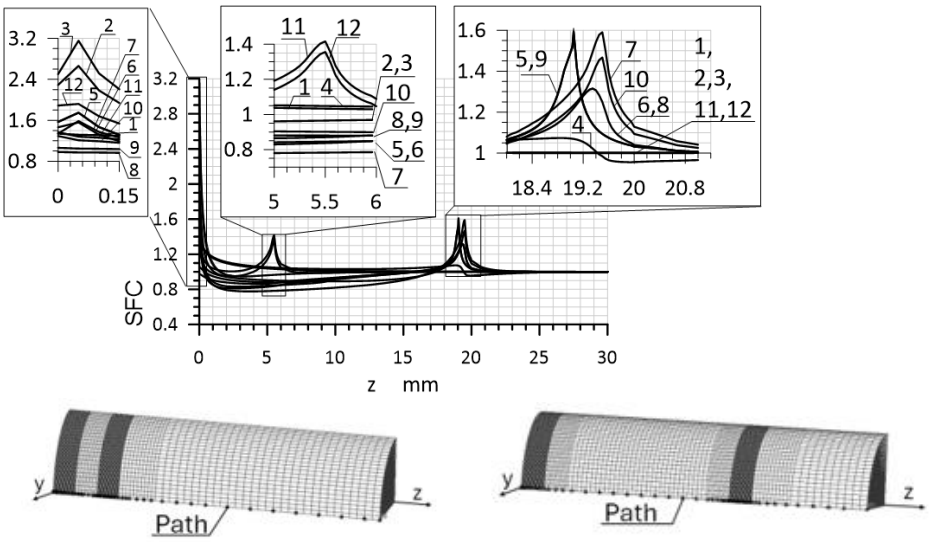

Fig. 6. SCF vs. z plots. Paths for calculating σ_z overlapped cylinder generator; paths for specimen immersed at 5 mm (left) and 20 mm (right)

PRE-PRINT ARTICLE
COPYRIGHT BY COMPOSITES THEORY AND PRACTICE JOURNAL
ISSN: 2299-128X

The lack of resin limited the occurrence of stress concentrations at the tip of the specimen (HDNs 1-3). The values were 2.29 and 3.16 for HDNs 2 and 3, respectively, while for HDN 1, it was 1.34. These results are in contradiction to those reported in [11]. In the latter, it was stated that the restriction in the side displacement of the specimen tip limited its side barreling and decreased the ESC. Nevertheless, restricting the side displacement of the specimen tip by gluing it to the cup bottom or imposing friction at the specimen end/cup bottom interface significantly deformed the specimen tip vicinity, Fig. 8a, resulting in a high local stress concentration. Notice that the profiles corresponding to the gluing connection and the presence of a significant friction overlay indicate much greater distortion than this one corresponding to the lack of friction.

The resin fillings produced both ESCs and MPSCs. They depended on the friction at the specimen/resin/cup interfaces and, to a lesser extent, on the immersion depth. The lowest and second lowest MPSCs occurred in the case of a lack of adhesion and friction (μ=0) at all the interfaces (HDN 4), and μ=0 at the cup-bottom/specimen-end interface and μ=0.5 at all the remaining interfaces (HDN 8), respectively. The highest MPSCFs that equal 1.59 occurred for the resin-filled cup with a convex resin meniscus, and a lack of friction at the cup-bottom/specimen-end interfaces (μ=0), as well as friction of μ=0.5 at the remaining interfaces (HDN 9). Assigning μ=0 to all the interfaces resulted in a drop in MPSCF to 1.43 (HDN 5). The assumption that the specimen, resin, and cup were glued (HDN 7) resulted in MPSCF being practically the same as in the case of HDN 9, i.e. 1.59.

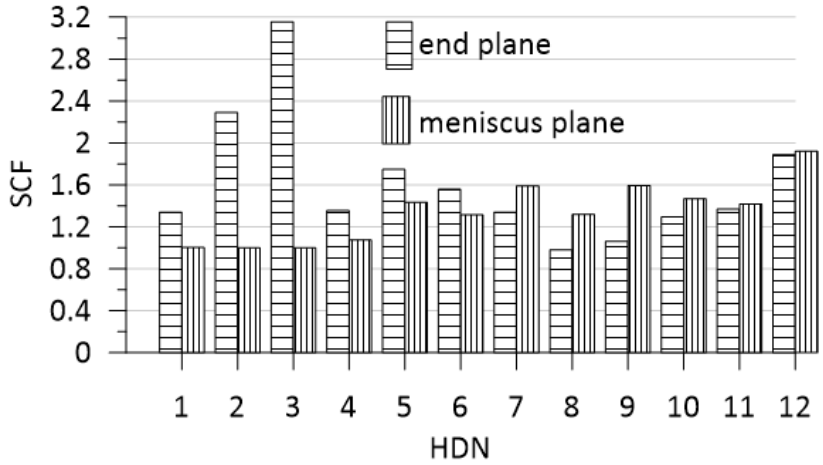

Fig. 7. Stress concentration factors. Numbers correspond to HDNs given in Table 1.

Comparison of the MPSCFs of HDNs 5 and 6 indicates that for the same interactions between the specimen, resin, and cup at the corresponding interfaces, the presence of a concave meniscus resulted in a lower value of the MPSCF than when a convex one was present. This phenomenon could be explained

PRE-PRINT ARTICLE
COPYRIGHT BY COMPOSITES THEORY AND PRACTICE JOURNAL
ISSN: 2299-128X

by comparing the deformations of the specimen sides occurring next to the convex and concave menisci, Fig. 8b.

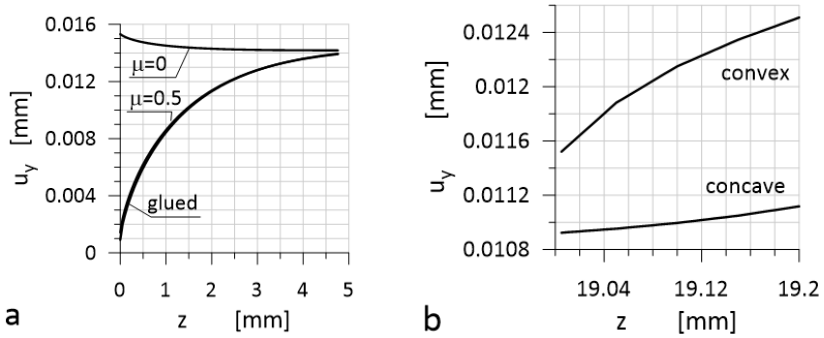

Fig. 8. Radial deformations of specimen: (a) near specimen tip, (b) next to convex and concave menisci.

Surprisingly, the concave meniscus produced a smoother transition of the specimen side deformation between the side restricted by the resin and the non-side-restricted specimen parts. It is known that such deformations enhance local fiber microbuckling and lower compressive strength [27, 28]. Reducing the specimen immersion to 5 mm, eliminating gluing, and assuming μ=0 at all the interfaces (HDN 11) reduced the difference between MPSCF and ESCF, slightly lowering the former and increasing the latter. An increase in the coefficient of friction to μ=0.5 (HDN 12) significantly raised MPSCF and ESCF, making the case the least favorable among those where resin filling was applied.

Since the results of the FE analysis showed that a complex stress state existed in the critical regions of the specimen, the SCF of one stress component was insufficient to judge which way of sample fixing would be most appropriate. Therefore, the results of all the specimen fixing variants were analyzed using the Tsai-Wu failure criterion, calculating the inverse strength ratio index (ISRI). The results are shown in Fig. 9.

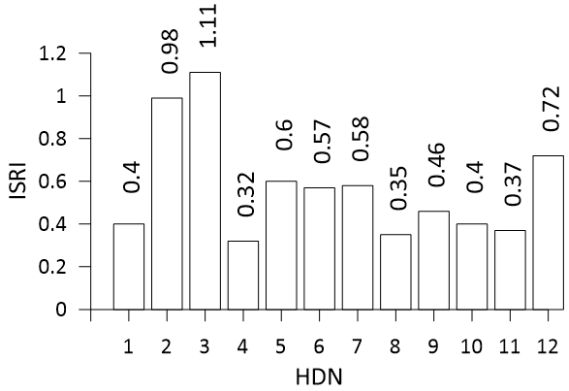

Fig. 9. Inverse strength ratio index

Since the loading was varied for each case, in such a way that $z = 0.5\ h_s$, the average longitudinal stress was approximately the same; the lowest ISRI was taken as the criterion for the holder choice. The lowest ISRI value was found for HDN 4, i.e. for the sample 20 mm immersed in the resin, with eliminated

PRE-PRINT ARTICLE
COPYRIGHT BY COMPOSITES THEORY AND PRACTICE JOURNAL
ISSN: 2299-128X

gluing and low friction at all the interfaces. Allowing a high coefficient of friction at the interfaces (HDN 6) resulted in a more than 77% growth in ISRI in relation to HDN 4. A similar result was noticed for HDN 7, i.e. when all the parts were glued, producing an ISRI higher by about 81% relative to HDN 4. This result implied that the gripping recommended in [9] should be avoided.

3.2. Experimental results

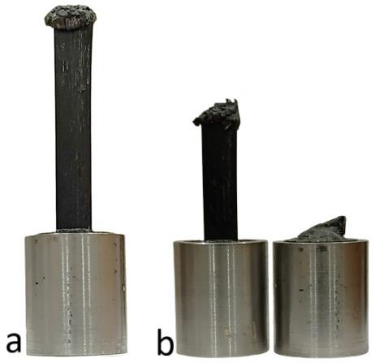

Fig. 10. Direct comparison of performances of IHD between 1 and 2 (top) and 7 (bottom) (a), and failure mode of specimen loaded using exclusively HDN 7 (b).

Figure 10a enables direct comparison of the performances of IHD and HDN 7 (completed per the recommendations in [11] and [9], respectively). One can notice that IHD was inferior since the failure of the specimen end free of surrounding resin occurred, while the one immersed in resin remained intact. In addition, two sets of three specimens were tested using each of the mentioned holders, the results of which are given in Table 5. It can be seen that the strength determined using IHD was much lower, again indicating the inferiority of this holder, which was in accordance with the results of the numerical analysis.

Table 5. Compressive strength experimental results

Holder design No.	
IHD	HDN 7
Strength N/mm^2	Strength N/mm^2
282.1	673.2
573.7	628.8
442.3	631.0
σ_{IHDav}=432.7	Σ_{HDN7av}=644.3

Since the elastic material properties assumed for the FE analysis differed from those of the materials used in the experiments, only a limited comparison could be made regarding the proportions of the

PRE-PRINT ARTICLE
COPYRIGHT BY COMPOSITES THEORY AND PRACTICE JOURNAL
ISSN: 2299-128X

average values of IHD and HDN7 obtained in the experiments against the proportions of the numerical values of HDN 1, HDN 2, and HDN 7. In principle, for linear systems, the ratio of the failure stresses should be inversely proportional to the ratio of the stress coefficient factors. The ratio of the average values corresponding to IHD and HDN 7 was $\sigma_{IHDav}/\sigma_{GDN7av} = 432.7/644.3 \approx 0.672$ (Table 5). On the other hand, the ratios of the calculated SCFs, i.e. the ratios of HDN 1 over HDN 7, and HDN 2 over HDN 7 were ESCF/MPSCF=1.34/1.59≈0.84 (1/0.84=1.187) and ESCF/MPSCF=2.39/1.59≈1.5 (1/1.5= 0.667), respectively. It means that the ratio of $\sigma_{IHDav}/\sigma_{HDN7av}$ fell in the range of the reciprocals of the ESCF/MPSCF ratios calculated for HDN 1 and GHDN 7, and calculated for HDN 2 and HDN 7. Referring to the discussion concerning HDN 1 and HDN 2 and the uncertainty concerning the assumed coefficient of friction values (sections 2.1 and 2.3), one could conclude that the experimental and numerical results were in reasonable agreement.

Analyzing the ISRI values, it could be concluded that the difference between the performances of HDNs 4, 8,10, and 11 was slight. Regarding those results, HDN 4 should be chosen; however, some crucial factors, e.g. friction, can change the preferences. Because of its strong influence on the results, the knowledge of the actual coefficient of friction is fundamental. Its value can be determined easily for calculation purposes; nevertheless, controlling it and reaching its repeatability, in practice, can be challenging. Therefore, before choosing the holder variant, a sufficient number of experimental setups should be made to gain confidence in friction control, and tested to obtain statistically significant results regarding the holder. The second important factor is the meniscus profile. The presence of a resin fillet positively impacts lowering stress concentration, as indicated by the numerical results obtained and the results presented in [29]. The meniscus profile should be as tangential as possible to the specimen wall. It implies good wettability of the specimen by resin, which can contradict the aim of avoiding resin adhesion to the specimen wall. Therefore, a release agent should be applied with care, and its excess should be avoided since it can produce a convex meniscus, increasing the stress concentration.

Conclusions

The performance of a hybrid holder designed for non-standard specimens of relatively large cross-sections, intended to determine the compressive strength of UD composites, was investigated numerically. The analyzed holder consisted of a metal cup filled with resin surrounding a specimen. The results showed that (i) concentrations of longitudinal stress occurred in two locations: at the tip of the specimen contacting the cup bottom and in the plane of the resin meniscus, (ii) the proportion between them could be controlled by (a) the presence or absence of adhesion between the resin and specimen, and resin and cup wall, (b) by friction at the mentioned interfaces and (c) by the specimen immersion depth. Eliminating adhesion and friction at the specimen/resin/cup interfaces decreased the differences in the values of the stress concentration factor present at the end of the specimen and in the meniscus

plane, indicating the possibility of optimizing the holder design. The analysis of all the results suggested that the HDN 4 solution would be the most suitable for industrial applications.

The advantage of the proposed design of specimen holder over standard ones lies in the fact that it is more suitable for the compressive testing of specimens with large cross-sections, if such tests are needed, than the latter. However, for each tested piece, two metal cups are needed as well as a fixture for their proper alignment, which is a primary drawback of this design.

Finally, it is worth noting that the differences between the HDN 4, 8, and 11 designs were found to be small. To confirm the correctness of the selection, experimental verification should be carried out using a sufficient number of specimens to make the results statistically significant. Therefore, future research will focus on this issue.

References

[1] Wisnom M.R., Size effects in the testing of fibre-composite materials, Compos. Sci. Technol. 1999, 59, 1937-1957

[2] Daniel I.M, Hsiao H.M., Is there a thickness effect on compressive strength of unnotched composite laminates? Int. J. Fract. 1999, 95, 143–158

[3] Haberle J., Strength and failure mechanisms of unidirectional carbon fibre-reinforced plastics under axial compression, PhD Thesis, 1991, Department of Aeronautics, Impoial College of Science, Technology and Medicine, 178

[4] Camponeschi G., The Effects of Specimen Scale on the Compression Strength of Composite Materials in Workshop on Scaling Effects in Composite Materials and Structures Compiled, Ed. Karen E. Jackson, November 15-16, 1993, NASA Conference Publication 3271, 81- 99

[5] Lee J., Soutis C., A study on the compressive strength of thick carbon fibre–epoxy laminates, Compos. Sci. Technol. 2007, 67**,** 2015–2026

[6] ASTM D695 Standard Test Method for Compressive Properties of Rigid Plastics

[7] ASTM D3410 Standard Test Method for Compressive Properties of Polymer Matrix Composite Materials with Unsupported Gage Section by Shear Loading

[8] ASTM D6641 Standard Test Method for Compressive Properties of Polymer Matrix Composite Materials Using a Combined Loading Compression (CLC) Test Fixture

[9] ISO 14126 Fibre-reinforced plastic composites — Determination of compressive properties in the in-plane direction

[10] SACMA SRM-1R-94 Compressive Properties of Oriented Fiber-Resin Composites.

[11] Chen T-K.: Compression Test Simulation of Thick-Section Composite Materials, MTL TR 92-25, Army Lab Command Watertown Ma. Material Technology Lab.

[12] Test Methods for Composites, a Status Report—Volume II: Compression Test Methods. Report No. *DOT*/*FAA*/*CT-93/17* II, FAA Technical Center, Atlantic City, NJ

[13] Camponeschi E.T., Jr., Compression Testing of Thick-Section Composite Materials, DTRC-SME-89/73, 1989

[14] Vankar S.R., Kaore A.N., Yerramalli C. S., Methodology for testing the compressive strength of pultruded composites, J. Reinf. Plast. Compos 2023, **45**, 544-557 doi.org/10.1177/07316844221133

[15] Thomsona D. et al., A study on the longitudinal compression strength of fibre reinforced composites under uniaxial and off-axis loads using cross-ply laminate specimens , Composites Part A: Applied Science and Manufacturing 2019, 121, 213-222

[16] Tarnopolskij J. M, Kincis T.J., Method of static investigations of reinforced *plastics*. Moscow: Chimia 1975.

[17] Coefficient of friction, rolling resistance and Aerodynamics., https://www.tribology-abc.com/abc/cof.htm (accessed 1.10.25)

[18] Liang S. et al., Estimation of the friction coefficient of the contact surface in CFRP anchor, Structures 2025, **77** 109200 https://doi.org/10.1016/j.istruc.2025.109200 (accessed 1.10.25)

[19] Eliezer Z., Schulz C. J., Barlow J. W., Friction and wear properties of an epoxy-steel system. Wear 1978, 46**,** 397-403

[20] Schon J., Coefficient of friction for aluminum in contact with a carbon fiber epoxy composite, Tribology International 2004, 395–404

[21] Dempsey J.P., Sinclair G.B.: On the stress singularities in the plane elasticity of the composite wedge. J. Elast. 1979, 9, 373-391

[22] Fedorov A.Y., Matveenko V.P., Numerical and applied results of the analysis of singular solutions for a closed wedge consisting of two dissimilar materials, Acta Mech. 2020231, 2711–2721, https://doi.org/10.1007/s00707-020-02668-w

PRE-PRINT ARTICLE
COPYRIGHT BY COMPOSITES THEORY AND PRACTICE JOURNAL
ISSN: 2299-128X

[23] Hui Ch-Y., Zhu B., Ciccotti M., Finite deformation field near the tip of a Blatz–Ko wedge bonded to a rigid substrate, Int J Fract. 2020, 238 71–87 https://doi.org/10.1007/s10704-022-00654

[24] https://www.fidelisfea.com/post/stress-singularities-at-reentrant-corners-a-fundamental-problem-in-fea (accessed 8.11.2025)

[25] https://www.ideastatica.com/support-center/singularities-vs-stress-concentration-area (accessed 8.11.20250)

[26] ANSYS Release 2024 R2, *ANSYS, Inc*

[27] Daum B., et al., A review of computational modelling approaches to compressive failure in laminates, Compos. Sci. Technol. 2019, 181107663

[28] Alves M. P., et al., Fiber waviness and its effect on the mechanical performance of fiber reinforced polymer composites: An enhanced review, Appl. Sci. Manuf. 2021, 149 106526

[29] Soutis C., Compression testing of pultruded carbon fibre-epoxy cylindrical rods, J. Mater. Sci. 2000, 34, 3441 – 3446